The authors thank the reviewer for his/her work and respect his/her opinion.

In the present document the comments given by the reviewer are addressed consecutively. The following formatting is chosen:

- The reviewer comments are marked in blue and italic.
- The reply by the authors is in black colour.
- Changed/extracted text sections are in green boxes.

A preliminary revised manuscript which incorporates the comments of both reviewers has been prepared. The made changes with respect to the 2nd reviewer are listed below. In this respect the authors would like to mention that the revised manuscript is now significantly larger than the indicative 30 to 40% requested in the Torque invitation.

"This paper presents some CFD results aiming to investigate the effect of trailing edge flaps on the aerodynamics of wind turbines. The paper is at the level of what is expected for a conference presentation but it lacks in originality, and depth to be considered as a journal publication.

To begin with, the paper is not presenting something new in terms of predictive aerodynamic methods, and it is not even applying existing methods in an innovative way. "

Previously published work on trailing edge flaps was in the large majority performed on the basis of blade element momentum methods, only very little is available on the basis of vortex models and CFD simulations were mostly performed on 2D airfoils. Only few papers are available for the 3D rotor which mainly addressed different objectives. This motivated the present 3D CFD studies.

In order to document this clearly, the introduction (Sect. 1, 2nd paragraph, line 13) was revised:

Over the last years several investigations showed the potential of the flap concept as for example a test on a full-scale turbine performed by Castaignet et al. (2014). In aero-elastic simulations fatigue load reductions up to approximately 30 % have been found for a trailing edge flap covering up to 25 % of the blade span of a 5 MW turbine (Barlas et al., 2012a). In most of the numerical studies the aerodynamic loading was computed by blade element momentum (BEM) codes (e.g. Bernhammer et al. (2016), Chen et al. (2017), Ungurán and Kühn (2016)), which have been extended with different engineering models to account for the unsteady flow (e.g. Bergami and Gaunaa (2012)). As viscous and unsteady aerodynamics have a great influence on dynamically deflected flaps (Leishman, 1994), it is however important to also apply higher fidelity models and gain knowledge of the flow physics. In this respect, a lot of studies have been performed on 2D airfoils, for example by Troldborg (2005) and Wolff et al. (2014) using CFD. 2D comparisons of simulation methods with different aerodynamic fidelities were performed by Bergami et al. (2015). For the 3D wind turbine rotor only few publications based on higher fidelity aerodynamic models are available. In 2012 Barlas et al. (2012b) compared CFD to BEM predictions for a rotor with trailing edge flap in an artificial half-wake scenario and found a reasonably good agreement with regard to the complexity of the test case. Leble et al. (2015) investigated trailing edge flaps on the 3D rotor and proved the load alleviation potential using a CFD approach. A recent benchmarking within the European Innwind.EU project (Jost et al., 2015a) showed however that there are still differences between the results of CFD simulations and BEM methods which need to be analyzed. While a previous investigation focused on the analysis of static flap deflection angles (Jost et al., 2016) by means of CFD, the main objective of the present work is to study the influence of unsteady 3D effects on the example of harmonically oscillating morphing flaps.

References:

Castaignet, D., Barlas, T., Buhl, T., Poulsen, N., Wedel-Heinen, J., Olsen, N., Bak, C., and Kim, T.: Full-scale test of trailing edge flaps on a Vestas V27 wind turbine: active load reduction and system indentification, Wind Energy, 17, 549–564, doi:10.1002/we.1589, 2014.
Barlas, T., van der Veen, G., and van Kuik, G.: Model predictive control for wind turbines with distributed active flaps: incorporating inflow signal and actuator constraints, Wind Energy, 15, 757–771, doi:10.1002/we.503, 2012a.
Bernhammer, L., von Kuik, G., and Breuker, R. D.: Fatigue and extreme load reduction of wind turbine components using smart rotors, Journal of Wind Engineering and Industrial Aerodynamics, 154, 84–95, doi:http://dx.doi.org/10.1016/j.jweia.2016.04.001, 2016.
Chen, Z., Stol, K., and Mace, B.: Wind turbine blade optimisation with individual pitch and trailing edge flap control, Renewable Energy, 103, 750–765, doi:http://dx.doi.org/10.1016/j.renene.2016.11.009, 2017.
Ungurán, R. and Kühn, M.: Combined individual pitch and trailing edge flap control for structural load alleviation of wind turbines, in: 2016 American Control Conference, doi:10.1109/ACC.2016.7525262, 2016.
Bergami, L. and Gaunaa, M.: ATEFlap Aerodynamic Model, a dynamic stall model including the effects of trailing edge flap deflection, Tech. rep., DTU - Technical University of Denmark, http://orbit.dtu.dk/files/6599679/ris-r-1792.pdf, 2012.
Leishman, J. G.: Unsteady Lift of a Flapped Airfoil by Indicial Concepts, Journal of Aircraft, 31, 288, doi:10.2514/3.46486, 1994.
Troldborg, N.: Computational study of the Risø-B1-18 airfoil with a hinged flap providing variable trailing edge geometry, Wind Engineering,
2, 89–113, 2005.
Wolff, T., Ernst, B., and Seume, J.: Aerodynamic behavior of an airfoil with morphing trailing edge for wind turbine applications, Journal of Physics: Conference Series, 524, http://iopscience.iop.org/article/10.1088/1742-6596/524/1/012018/pdf, 2014.
Bergami, L., Riziotis, V., and Gaunaa, M.: Aerodynamic response of an airfoil section undergoing pitch motion and trailing edge flap deflection: a comparison of simulation methods, Wind Energy, 18, 1273–1290, doi:10.1002/we.1759, 2015.
Barlas, T., Zahle, F., Sørensen, N., Gaunaa, M., and Bergami, L.: Simulations of a rotor with active deformable trailing edge flaps in half-wake inflow: Comparison of EllipSys 3D with HAWC2, in: European Wind Energy Conference (EWEC), 2012b.
Leble, V., Wang, Y., and Barakos, G.: CFD analysis of 10-MW turbines, in: German Wind Energy Conference (DEWEK), 2015.
Jost, E., Barlas, T., Riziotis, V., and Navalkar, S.: Innwind D2.3.2 - Validation of New Control Concepts by Advanced Fluid-Structure Interaction Tools, Tech. rep., Innwind.EU project, 2015a.

The intention of the present paper is to demonstrate that the deflection of the flap on the 3D rotor causes a complex wake development and induction which influences the aerodynamic loads over large parts of the blade. This knowledge is essential for the development of smart rotors and also improved wake models. As a matter of fact the present work and similar simulations were used for the verification of aerodynamic engineering models in BEM within the European projects Innwind.EU and AVATAR. In this background the authors are not aware of any similar study for large wind turbines, but would appreciate any indications.

"In addition, the depth of the presented analysis of the effect of trailing edge flaps on the 3D unsteady aerodynamics of a wind turbine is at least superficial. The authors compare 2D and 3D results for the flapped wind turbine section but this comparison is not enough to provide a detailed understanding of how much the trailed vorticity and the additional edge effects of the finite span flap can be quantified in a way that engineers can use for practical calculations. "

We agree with the remark that further studies are required to quantify the effect of trailed and shed vorticity in more practical way. The objective of the present work is to investigate the underlying flow phenomena, identify the dominant aerodynamic effects and consequently provide the basis to derive such models. In this respect, the last paragraph of Sect 4.4 of the original paper was revised to clarify the content.

The comparison of the 2D and 3D lift amplitudes shows the expected reduction due to the influence of trailing vortices. The 3D lift amplitude alleviates to 66-73% of the result of 2D simulations at the same flap frequency based on the rounded values listed in Table 4 (in original manuscript: Table 3). As it was noticed before in Sect. 4.1 with regard to the thrust oscillation, the lift amplitude of the 3p and 6p case is similar. This is also seen in the relative amplitude reduction, as 3p shows a significantly lower value than the other cases. Unfortunately, the reason for this phenomenon could not finally be clarified since this would require a method to extract the AoA in transient cases. This would allow to judge and compare the AoA oscillation between all 3D cases, which provides further insight. Further research is required in this respect. Nevertheless, this relative reduction is roughly constant throughout all flap frequencies. An earlier investigation (Jost et al., 2016) focused on the impact of steady flap deflections on the blade performance. Various flap extensions along the blade radius (10% and 20%) and chord (10% and 30%) were analyzed in a parametric study at 15 m/s wind speed. The analysis included also a comparison to 2D simulations and an extract of the results is shown in Table 6 for positive and negative deflections.

Table 6. ***c_l amplitude, 75% blade cut, 15 m/s, steady deflections (Jost et al., 2016)***

	$\beta = 10°$		$\beta = -10°$	
	10% chord	30%chord	10% chord	30%chord
$\Delta c_{l,3D,10\%span}/\Delta c_{l,2D}$	70%	69%	65%	65%
$\Delta c_{l,3D,20\%span}/\Delta c_{l,2D}$	80%	79%	75%	77%

A correlation to the results of the present study can be noticed. The relative amplitude reduction ($\Delta c_{l,3D,10\%span}/\Delta c_{l,2D}$) is very similar for both chord extents and in a comparable range as observed in the oscillating cases. Please note that the slightly lower values for steady deflections can be explained by the adjusting axial induction as described in Sect. 4.2. The value for 20% radial extent ($\Delta c_{l,3D,20\%span}/\Delta c_{l,2D}$) is in contrast about 10% higher. Consequently, the relative lift amplitude reduction at mid flap position $(\Delta c_{l,3D}/\Delta c_{l,2D})_{mid,flap}$ can serve as a rough characteristic value for a certain flap layout. It also allows a decoupled consideration of 3D and unsteady effects at this location. This means that as a first estimation $(\Delta c_{l,3D}/\Delta c_{l,2D})_{mid,flap}$ can be determined based on a 3D simulation with static maximum flap deflection. The amplitude reduction by shed vorticity can be investigated separately in 2D and can then be superimposed with the 3D result. This simplified or quasi-2D approach with regard to shed vorticity is however only valid at the mid flap area. Closer to the flaps edges the unsteady effects will also become three-dimensional.

"After all the CFD computations the reader expects some model/table/equation that will be transferable to other cases. Otherwise this work will have to be repeated for any other wind turbine and for any other flap location apart from the selected one here."

With regard to an analytical model description, the CFD results suggest the consideration of trailing and shed vorticity in the turbine near wake. This approach is followed by several researchers, e.g.:

- M. Aparicio et al. (http://dx.doi.org/10.1088/1742-6596/753/8/082001)
- G. Pirrung et al. (http://dx.doi.org/10.1002/we.1969)

A first comparison to the present work is performed in:

- Barlas et al. (http://doi.org/10.1088/1742-6596/753/2/022027)

Similar comparisons were performed in the AVATAR project and can be found in:

- Deliverables of work package 3 (D3.1, D3.2, D3.3), (www.eera-avatar.eu/publications-results-and-links)

The authors agree that this was not accurately documented in the original manuscript. The following text is added to section 4.4:

With respect to a more general aerodynamic modelling in lower fidelity tools the present investigation suggests a simplified consideration of near wake effects. The dominant phenomena could be assigned to trailing and shed vorticity which can be captured by such approaches. First comparisons of the present simulations to the near wake model by Pirrung et al. (2016) can be found in (Barlas et al., 2016). Aparicio et al. (2016a) have also published favorable results following a similar approach. Further benchmarks were performed within the AVATAR project (Ferreira et al. (2015), Aparicio et al. (2016b)).

"More interestingly, the paper is not considering the simple fact that once a flap is deployed, it will begin to affect the sectional pitching moments, it will lead to different displacement and perhaps torsion of the section and this will result in a different behavior than what is shown in the paper. For the large flexible blades of wind turbines, including the effect of aeroelasticity is important and this effect is neglected in this paper."

The authors agree that the pitching moment and aero-elasticity is important when trailing edge flaps are applied on a wind turbine rotor. Especially when it comes to assessing the overall performance of the flap concept, this is essential.

The focus of the present work is to study the aerodynamic effects of the flap and provide a basis for the derivation of simplified engineering models. In this respect, aero-elasticity is deliberately neglected to capture solely flap effects. As written by the reviewer, in an aero-elastic simulation the blade flapping and torsion would lead to an overlapped plunging and pitching motion of the airfoil. A distinction between the different aerodynamic effects is then difficult.

In order clarify the intentions of the present work, the following has been added to the end of Sect. 1:

It shall be noted that the present work does not aim towards an assessment of the flap concept. The objective is to investigate unsteady 3D aerodynamic effects caused by trailing edge flaps and to obtain deeper knowledge about the dominant phenomena as fundamental basis for an enhancement of engineering tools commonly used for load calculations. Within this respect aero-elasticity is not considered since on a flexible blade pitching and plunging movements are superimposed to the flap oscillation and a distinction of the isolated effects is difficult.

Additionally an outlook is added to the conclusion (Sect. 5):

As discussed in the present study, an overall CFD-based assessment of the flap concept requires the incorporation of aero-elasticity. On a flexible blade the flap oscillation will be superimposed with pitching and plunging motions. A careful evaluation of these phenomena in comparison to the present investigation will allow an isolation of the different effects and lead to a deeper insight of 3D characteristics of trailing edge flaps on a real wind turbine rotor.

The evaluation of the pitching moment is added to the paper. For this, the following modifications have been made to the revised manuscript:

- Section 2.1 is added to introduce the aerodynamic effects of the flap on c_l, c_d and c_m. As by this section 2 has become consequently more elaborate, it is divided in three subsections. (1. 2D airfoil, 2. 3D rotor blade, 3. Theodorsen theory)

2.1 **2D airfoil**

Trailing edge flaps are able to increase or decrease the airfoil lift for respectively positive (downwards) or negative (upwards) deflections due the change of the airfoil camber. As exemplarily displayed in Fig. 1 this leads to a vertical shift of the lift coefficient c_l over angle of attack (AoA) α curve. This possible lift increase is however mostly connected to an increase in drag as depicted in the drag coefficient's c_d-α plot. Additionally the moment coefficient around the quarter chord point c_m is also significantly influenced by the change of the airfoil shape. In general the flap concept aims towards reducing the overall load fluctuation, but in particular the dominant out-of-plane forces and blade root bending moment. They are primarily influenced by the lift coefficient.

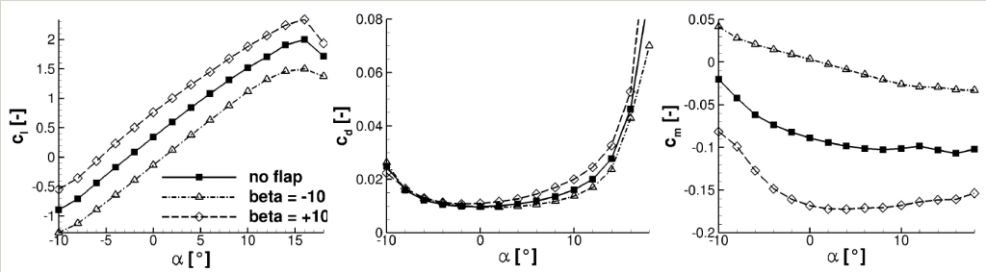

Figure 1. **Example of flap deflection on c_l, c_d and c_m (FFA-w3-241 airfoil, Reynolds number Re = 15.57e6, Mach number M = 0.2)**

2.2 **3D rotor blade**

The increase or decrease of lift in a blade section with trailing edge flap influences the aerodynamic phenomena in most parts of the rotor blade. …

- Section 2.3: Reference to Hariharan and Leishman (1996)

Additionally to the lift equation, Theodorsen developed functions for c_m, the pressure drag c_{dp} and the flap hinge coefficient $c_{m,fh}$. It is referred to Hariharan and Leishman (1996) for their definition. …

References:

Hariharan, N. and Leishman, J.: Unsteady aerodynamics of a flapped airfoil in subsonic flow by indicial concepts, Journal of Aircraft, 33, 855–868, doi:http://dx.doi.org/10.2514/3.47028, 1996.

- Section 3.5: Evaluation of the influence of time step on the local torsion moment

Figure 8 shows the resulting driving force, thrust and torsion moment variations at mid flap position. The torsion moment is evaluated relative to the blade pitch axis and positive reducing the blade pitch. The forces and moment are normalized with the total mean value to allow an easier assessment of the differences. While thrust and torsion moment show a good agreement for nearly all time step sizes, higher deviations are observed in the driving component in which the drag differences have a stronger impact. However, a convergence of the curve progressions with decreasing time step size can be observed leading to small differences between 0.125° and 0.25°.

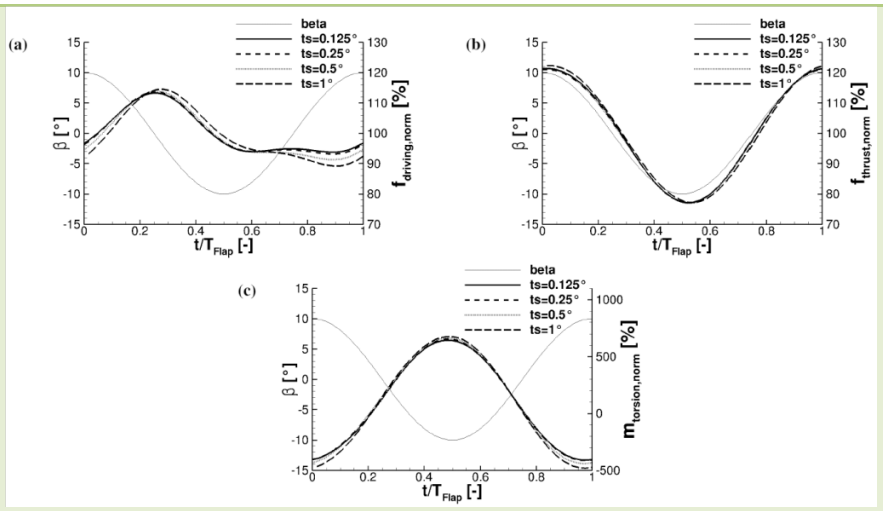

Figure 8. **3D influence of time step, 6p, 75% blade cut, normalized driving force (a), thrust (b) and torsion moment (c)**

- Section 4.1: Sectional torsion moment is added at 75% blade cut and along the blade radius

In the following, like in the time step study, the 75% cut as mid flap position was extracted from the simulations. Figure 11 shows the results of the local driving force, thrust and torsion moment at this location over one flap period for all simulated frequencies.

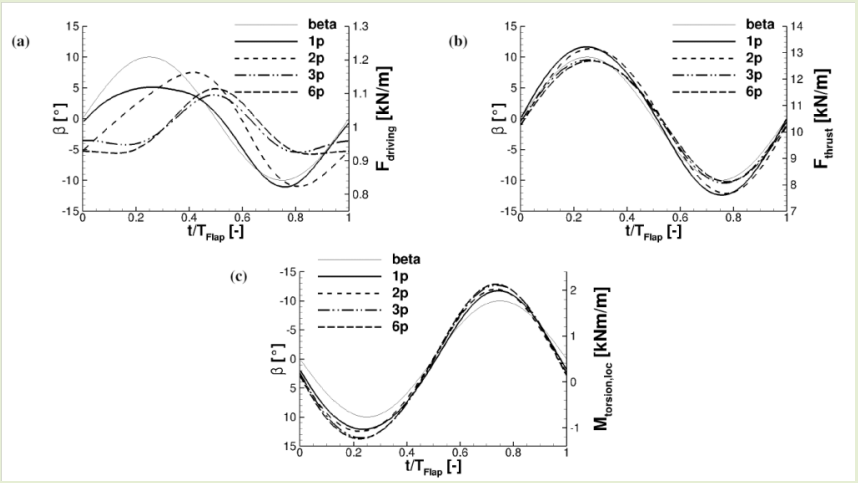

Figure 11. **Variation of flap frequency, 75 % blade cut, driving force (a), thrust (b) and local torsion moment (c)**

…

Please note that in the plot of the local torsion moment (Fig. 11c) the β-axis is reversed in order to be able to better judge the phase shift. The moment shows an increase of amplitude with increasing flap frequency, mainly between the 2p and 3p case like it was observed vice versa for thrust. The high frequencies 3p and 6p are again similar. All curves show a lead with respect to the flap signal. A more detailed elaboration of the torsion moment relative to the quarter chord point is also performed in Sect. 4.4.
In Fig. 12 and Fig. 13 sectional distributions of driving force, thrust and torsion moment over the blade radius are shown for 1p and 6p case respectively. Four instantaneous solutions are plotted for maximum, minimum and 0° flap deflection. …

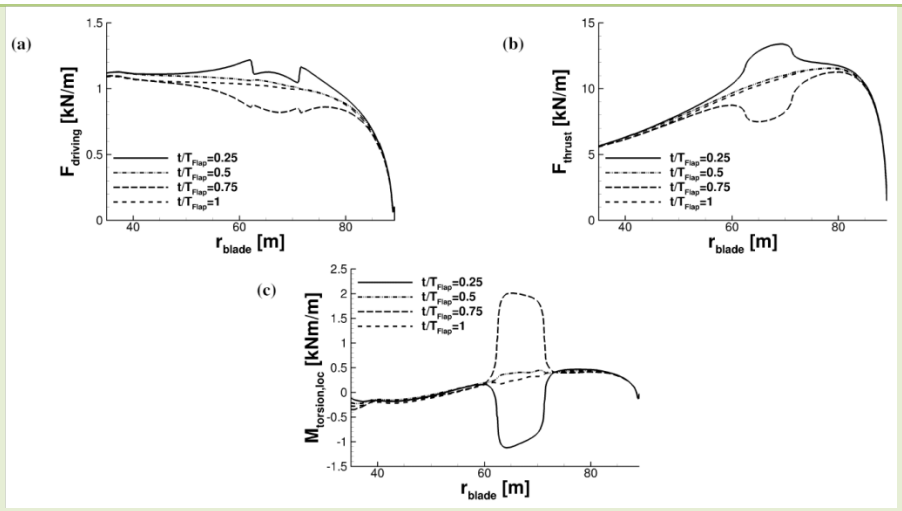

Figure 12. **1p sectional forces (driving force (a), thrust (b) and local torsion moment (c))**

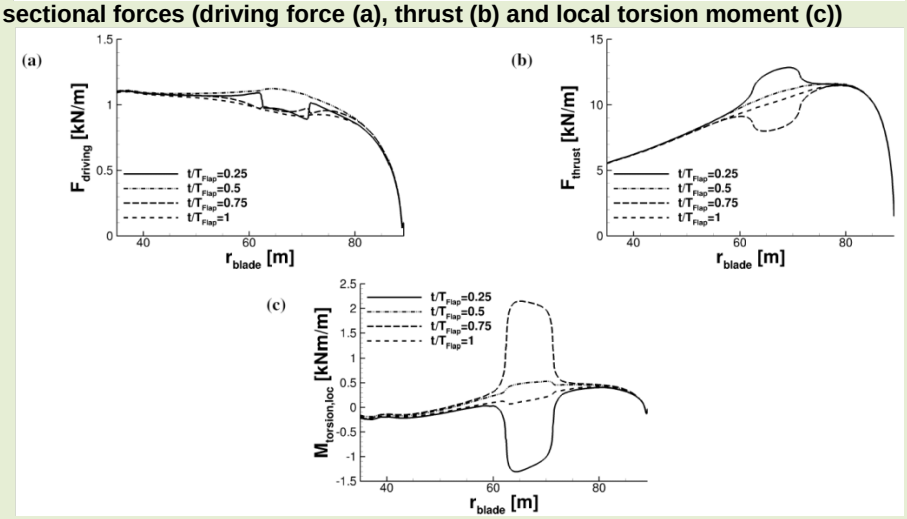

Figure 13**. 6p sectional forces (driving force (a), thrust (b) and local torsion moment (c))**

… With regard to the torsion moment around the pitch axis a strong oscillation is seen in flap section with steep gradients at the flap edges. This torsion moment or c_m oscillation is typical for trailing edge flaps (Ferreira et al., 2015) and its effect on the overall performance of the flap concept needs to be investigated separately in an aero-elastic simulation when the blade is able to twist.

- Section 4.4: 2D /3D comparison of torsion moment at quarter chord point.

The results of the moment coefficient c_m are depicted in Fig. 21 for the 1p and 6p frequency. It is noted that while the previous plots of the 3D torsion moment were evaluated relative to the pitch axis, the results have been transferred to the quarter chord point for the 2D comparison. In general only a minor influence of unsteady aerodynamic effects is observed. A slight reduction of the amplitude and small hysteresis is seen in the 3D case. The 2D results are in a good agreement to (Ferreira et al., 2015), for which similar simulations have been performed for the same airfoil.

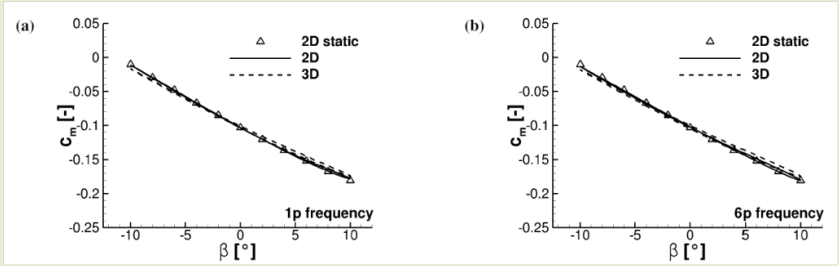

Figure 21. ***Comparison of 2D/3D moment coefficient for different flap frequencies: 1p (a), 6p (b)***

- Section 5: Conclusions are appended.

… Additionally less hysteresis is seen at the rotor blade which is connected to the decrease of lift amplitude. 2D and 3D results regarding the moment coefficient were also compared and exhibited an only minor influence of unsteady effects.

"In conclusion, I feel that the authors are on the right track but they have to investigate thing deeper, collect a volume of work that covers several cases and try to summarise the effects of the flap in a consolidated way in a model. Their work and method are good but they are simply not there yet to be able to provide the depth of analysis required by an archival journal publication."

Thank you. The authors aim towards a deeper investigation in the revised manuscript. Exemplary two extracts are shown here.

- Section 4.1: Elaboration with regard to sectional force distributions

In Fig. 12 and Fig. 13 sectional distributions of driving force, thrust and torsion moment over the blade radius are shown for 1p and 6p case respectively. Four instantaneous solutions are plotted for maximum, minimum and 0° flap deflection. Thrust shows the expected increase and decrease in the flap section with a smooth load distribution over the flap edges. This smoothing is a consequence of the positive effect of the flap deflection on neighboring blade sections as described in Sect. 2.2. While trailing vorticity reduces the effect of the flap in the flap section compared to 2D, the sections next to the flap part produce higher/lower lift due to the induced upwash/downwash for respectively positive/negative flap angles. The change of sign in induced velocity caused by the flap edge vortices is also apparent in the driving force as significant steps are appearing at the transition between flap and rigid rotor part. An opposite behavior of sectional driving force in relation to thrust can be noticed by comparing the diagrams. When thrust increases locally in the flap area, the driving force decreases in relation to neighboring sections. This results again from the strong influence of drag on the driving component at rated wind turbine conditions and will be explained on the basis of 1p case as follows. Due to the low reduced frequency in this case (k = 0.024), the influence of shed vorticity is still weak. For maximum positive deflection (t/T_{Flap} = 0.25) the increase of trailing vorticity causes a downwash in the flap section. This reduces the effective AoA and leads to a rise of induced drag in addition to the drag augmentation caused by the flap deflection itself. The overall drag increase is compensated by the lift increase resulting from the flap deflection and relative to 0° flap deflection an increase of driving force is achieved. The neighboring sections to the flap experience an additional upwash in case of positive deflections. Consequently, the induced drag reduces associated with the lift increase and these sections produce in total a higher sectional driving force. Similar observations are made vice versa for maximum negative deflections, but the driving force increase in the flap section is less pronounced compared to the decrease in case of positive deflection. Further elaborations in this respect can be found in Sect. 4.3, in which lift and drag forces are extracted and compared. With regard to the torsion moment around the pitch axis a strong oscillation is seen in flap section with steep gradients at the flap edges. This torsion moment or c_m oscillation is typical for trailing edge flaps (Ferreira et al., 2015) and its effect on the overall performance of the flap concept needs to be investigated separately in an aero-elastic simulation when the blade is able to twist.

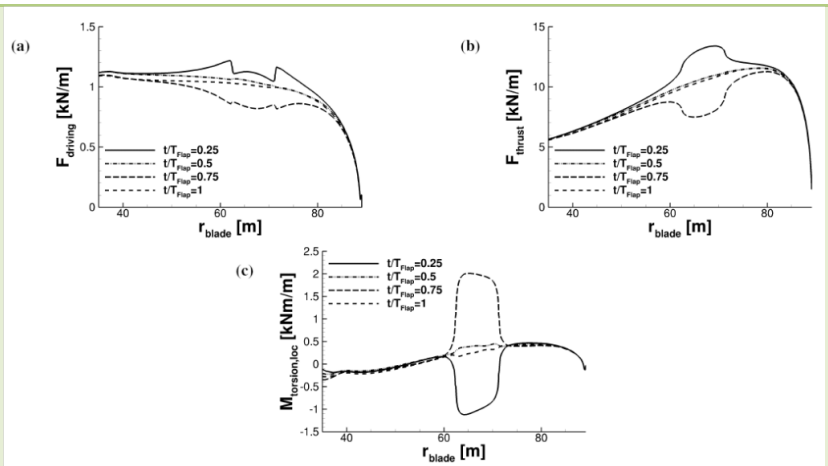

Figure 12. **1p sectional forces (driving force (a), thrust (b) and local torsion moment (c))**

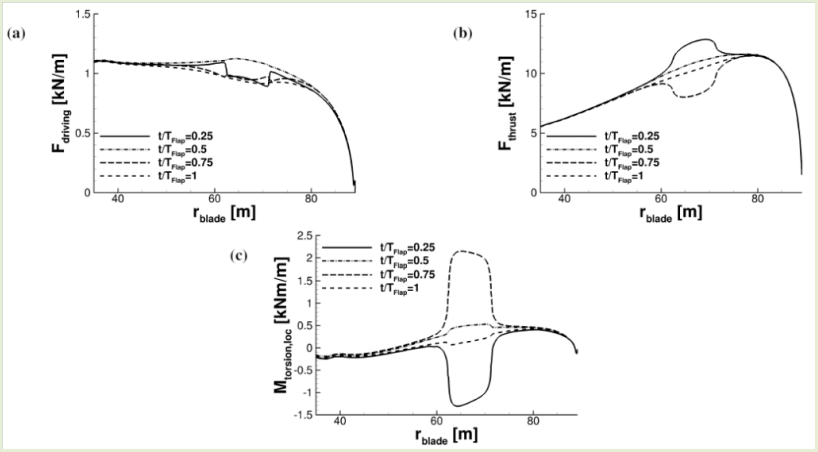

Figure 13. **6p sectional forces (driving force (a), thrust (b) and local torsion moment (c))**

- Section 4.3: General revision of section 4.3, also in connection to comments by the first reviewer

4.3 **Influence of varying AoA in 3D**

As observed in the previous section, in the 3D rotor case the local AoA is oscillating over a flap period as a result of dynamic inflow. This means from an aerodynamic point of view that two unsteady mechanisms are superimposed: pitch and flap oscillation. The objective of the present work is though to characterize and quantify unsteady 3D effects solely due to flap deflection and consequently some preliminary considerations have to be made. For this purpose the 1p frequency is regarded in the following, for which quasi-steady assumptions are eligible and the reduced axial velocity method can be applied. The variation of the local inflow velocity and the AoA is shown in Fig. 17 for the mid flap position. While the inflow velocity shows no major variations, the AoA oscillates with an amplitude of 0.6°.

When the instantaneous AoA is extracted from the 3D simulation it includes the oscillations caused by both mechanisms, dynamic inflow and flap oscillation. The dynamic inflow oscillation represents an oscillation of the baseline AoA as a result from the variation of the axial induction of the turbine. In contrast the oscillations caused by the flap originate from the downwash of 3D trailing vorticity which changes the effective AoA. As the objective is to quantify 3D trailing vorticity, the flap-caused AoA oscillation should be mimicked to the aerodynamic coefficients, while in theory the influence of the dynamic inflow caused oscillation should be eliminated. A clear distinction between both oscillations is however not possible and requires further aerodynamic modelling. Nevertheless, the influence of the overall AoA oscillation on the 3D extracted aerodynamic coefficients can be assessed.

Figure 18 presents the resulting c_l and c_d variations in addition to the resulting variations for an averaged angle of attack of 6.5° and local inflow velocity of 68 m/s ($c_{l,mean}$, $c_{d,mean}$). The moment coefficient c_m is not dependent on the inflow direction so that the evaluation of the

AoA uncertainty for the c_m behavior can be excluded in this section. It can be seen that the AoA oscillations have only a minor influence on the value of c_l but strong on c_d. This is reasonable as for the determination of c_l and c_d in the 3D case, the forces are integrated from the surface solution as driving force and thrust components at first and then transferred to the local inflow or also called aerodynamic coordinate system. The procedure is shown in Fig. 19 for both components. To determine total lift and drag forces both shares by driving force and thrust are summed up. As the value of c_l is roughly 100 times larger compared to c_d, a projection difference of 0.6° as observed in the 1p case has only a negligible impact on c_l. Consequently the results for c_l and $c_{l,mean}$ are very similar. c_d and $c_{d,mean}$ differ strongly. Based on the previous considerations this difference consists of two parts, induced drag which originates from trailed vorticity and the drag resulting from the AoA oscillation caused by dynamic inflow.

The plot in Fig. 18 can be directly linked to the curves for driving force and thrust in the 1p case displayed Fig. 11 (in original manuscript: Fig. 10) and Fig. 12 (in original manuscript: Fig. 11). Thrust is dominated by c_l and consequently the progressions over a flap period are very similar. The driving component is a superposition of both forces which are oscillating at a different phase. This can be noticed for example at the time instance when the flap is deployed to maximum deflection (t/T_{Flap} = 0.25). c_l but also $c_{d,mean}$ is maximal and as a result the progression of driving force flattens. Vice versa the phenomenon is observed at minimum deflection (t/T_{Flap} = 0.75).

With regard to the objective of this section, determining the influence of the AoA oscillation on the 3D extracted aerodynamic coefficients, it can be concluded that the extracted c_l is only minor affected and it is eligible to use $c_{l,mean}$ for the comparison to 2D simulations and the evaluation of the impact of trailing vortices. With respect to c_d it is difficult to clearly distinguish between the part caused by the AoA oscillation and the induced drag from trailed vorticity. In order to judge the impact of trailing vortices on c_d, this differentiation is however necessary and the part caused by the AoA oscillation needs to be eliminated. The emphasis of the comparison to 2D simulations is hence on lift and moment coefficient.

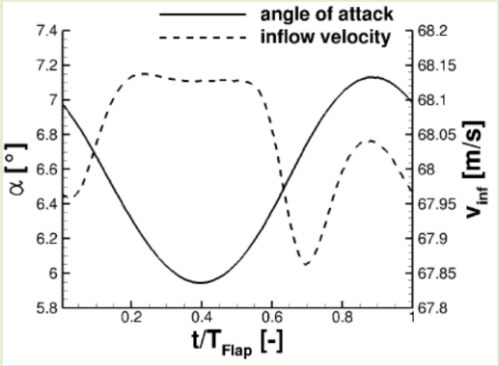

Figure 17. **1p instantaneous inflow conditions 3D, 75 % radius**

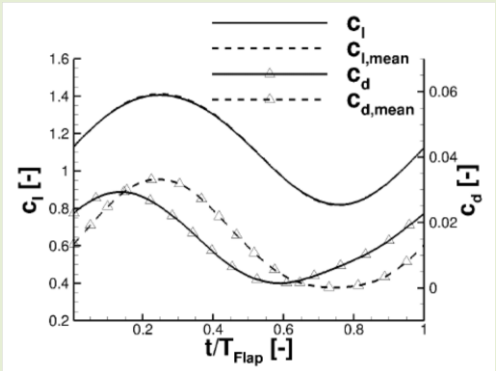

Figure 18. **1p comparison of lift and drag, 3D instantaneous/ 3D mean, 75 % radius**

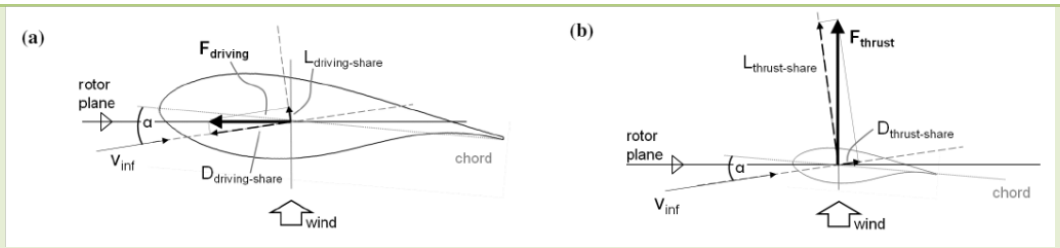

Figure 19. **Transformation of driving force and thrust to local aerodynamic coordinate system (driving force (a) and thrust (b))**

In addition to the above changes, two smaller corrections had to be performed by authors for correctness:

- Table 2, original manuscript: An error was found in post-processing for β=0° (evaluation of wrong revolution) which changed the results to a power of 10.71MW (reduction by 0.37%) and to a thrust of 1790kN (reduction by 0.17%). The conclusions are unaffected.
- Table 3, original manuscript: corrected typo for (∆cl,3D /∆cl,2D) to 73%